

Article pubs.acs.org/JPCC

Enantioselective Effects in the Electrical Excitation of Amine Single-**Molecule Rotors**

Tedros A. Balema, Yilang Liu, Natalie A. Wasio, Amanda M. Larson, Dipna A. Patel, Prashant Deshlahra,* and E. Charles H. Sykes*



Cite This: J. Phys. Chem. C 2021, 125, 3584-3589



ACCESS I

Metrics & More

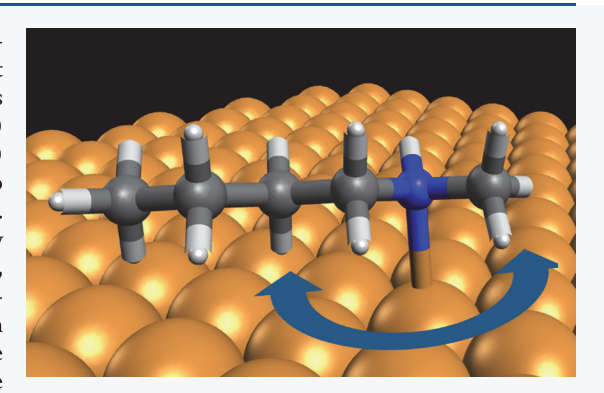


Article Recommendations



Supporting Information

ABSTRACT: This paper describes a single-molecule study of Nmethylbutylamine molecular rotors supported on a Cu(111) surface. It is first demonstrated that the chirality of the individual rotating molecules can be directly determined by scanning tunneling microscopy (STM) imaging and understood with density functional theory (DFT) simulations. Tunneling electrons from the STM tip are then utilized to excite vibrational modes of the molecule that drives the rotational motion. Experimental action spectra were used to demonstrate that the electrically induced rotational motion of N-methylbutylamine occurs above 360 meV, which coincides with C-H stretching vibrational modes. The measurements also reveal that, above this 360 meV threshold, the excitation occurs via a one-electron process. DFT calculations indicated that the rotation barrier is over an order of magnitude smaller, meaning that the rotor is excited via high-energy vibrational modes that then couple to the



low energy rotational mode. Furthermore, by adjusting the electron flux, individual rotational motions between the six different stable orientations of the molecule on the Cu(111) surface were monitored in real time. It was found that, for most STM tips used to electrically excite the rotors, the rotation of one enantiomer is faster than the other. This confirms an earlier report that STM tips can themselves be chiral and illustrates the fact that diastereomerism arising from a chiral STM tip interacting with a chiral molecule can lead to significant physical differences in the rotation rates of R versus S molecular rotors. This result has ramifications for interpreting the data from experiments where nanoscale electrical contacts to chiral molecules are made in devices like break junctions and scanning probe experiments.

■ INTRODUCTION

Molecular rotors, motors, and machines are of current interest, and the recent literature contains many reports of organic molecular structures and their functionality in a range of chemically, thermally, or photon-driven processes. 1-10 Considering that molecular machines found in nature operate at interfaces, it is important to study surface-bound systems. 11-21 However, factors such as friction, thermal fluctuations, intramolecular bonding, and steric effects have imposed various challenges in understanding many surface molecular machines. 11,22 To address these gaps in understanding, scanning tunneling microscopy (STM) offers the unique ability to make single-molecule measurements of molecular rotation on surfaces and to interrogate the details of electroninduced molecular motion at the nanoscale. 23-31 Thanks to this approach, there have been important breakthroughs in studying molecular machines such as electrically driven nanocars, 32 synchronized molecular motor networks, 33 and single-molecule motors. 27,34 While still far from application, molecular rotors offer an ideal test bed for the investigation of how a molecular structure affects dynamical motion. Related to

the current work, combining STM and density functional theory (DFT) calculations has led to a deeper understanding of thioether-based single-molecule rotors and motors. 27-31,35,38 Specifically, electrically induced directional motion is only possible when the adsorbed rotor is chiral via activation of vibrational modes by tunneling electrons as opposed to thermally activated rotors in which second law thermodynamics dictates that they must exhibit a random motion.^{27–31,35,37}

This paper describes a single-molecule study of the rotational motion of chiral N-methylbutylamine rotors supported on a Cu(111) surface. Comparing the relative rotational rates of the chiral N-methylbutylamine molecular rotors induced by inelastic tunneling electrons, it was observed

Received: December 1, 2020 Revised: January 22, 2021 Published: February 5, 2021





that there was a strong enantioselective coupling between the STM tip and the adsorbed chiral molecule leading to large differences in the electrically excited rotation rates in *R* and *S* molecular rotors.

■ EXPERIMENTAL METHODS

Low-temperature (STM) LT-STM was operated with a base pressure of $<1\times10^{-11}$ mbar. N-Methylbutylamine was acquired from Sigma Aldrich at 95% purity and further purified by degassing with multiple freeze/pump/thaw cycles. N-Methylbutylamine was then vapor-deposited onto a Cu(111) sample held at 5 K using a collimated molecular doser attached to a precision leak valve. Anneals in the 80–120 K range were performed to equilibrate the molecules by removing the sample from the cryogenically cooled stage of STM and placing it into a sample holder held at room temperature in an ultrahigh vacuum (UHV) chamber for a predetermined time period. The crystal was then cooled back to 5 K by putting it back into the STM stage for high-resolution imaging and spectra collection. Etched W STM tips were used in this study.

■ COMPUTATIONAL DETAILS

Periodic density functional theory (DFT) calculations were performed within the Vienna *ab initio* simulation package (VASP) using the Perdew–Burke–Ernzerhof (PBE) exchange correlation functional based on generalized gradient approximation (GGA). $^{38-41}$ Plane-wave basis sets used to approximate wavefunctions of valence electrons were expanded to a 400 eV kinetic energy cutoff. The interactions of valence electrons with atom cores were described by the projector-augmented wave (PAW) method. Electronic structures were converged self-consistently to energy differences less than 1×10^{-8} eV between successive steps. All surface and bulk metal calculations were performed without spin polarization.

The Cu(111) surface was represented using a four-layer 4 Cu × 4 Cu supercell with about six layers of vacuum space between neighboring slabs along the [111] direction. The supercell sizes are defined to be $10.28 \times 10.28 \times 20.98 \text{ Å}^3$ based on the PBE-optimized Cu lattice constant (3.634 Å). The lower two-layer Cu atoms were fixed at the bulk positions, and the upper two-layer Cu atoms were relaxed. The longrange interactions among neighboring slabs of Cu were corrected using dipole moments along the [111] direction.⁴³ All calculations were performed using a 2 × 2 × 1 Monkhorst-Pack k-point mesh.⁴⁴ The initial structure of N-methylbutylamine adsorbed on the Cu(111) surface was optimized until forces on atoms were less than 0.02 eV Å⁻¹. Rotational barriers and shapes of potential energy surfaces for the rotation were derived within the rigid-rotor approximation using single-point calculations on images formed by rotating an optimized structure from 3 to 66° in 3° intervals, with the axis of rotation perpendicular to the Cu(111) surface and centered at the Cu atom underneath the N atom. The rigid-rotor calculation for the intact rotor is compared to a nudged elastic band calculation in the Supporting Information (Figure S4).

■ RESULTS AND DISCUSSION

Figure 1 shows a summary of STM data of N-methylbutylamine deposited on Cu(111) at 5 K and annealed to 80 K to equilibrate the system. Figure 1A shows a schematic of the molecular adsorption site of N-methylbutylamine and illus-

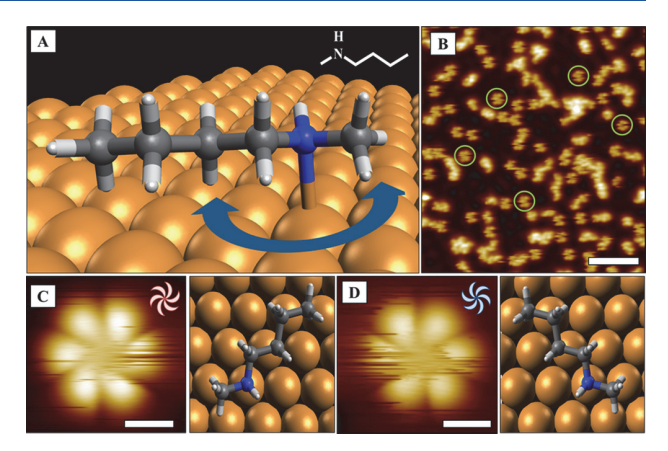


Figure 1. (A) Schematic of surface-adsorbed N-methylbutylamine on Cu(111). The rotational behavior of the amine rotor around the N—Cu "axel" is highlighted with a blue arrow. (B) Large-scale 5 K STM image of surface-adsorbed N-methylbutylamine on Cu(111). The green circles are representative examples of the isolated rotor molecules used in the study. Imaging conditions: 10 mV, 90 pA. Scale bar: 5 nm. High-resolution STM images of accompanying topview models of the (C) R enantiomer of an N-methylbutylamine molecule adsorbed on Cu(111) and the (D) S enantiomer of an N-methylbutylamine molecule adsorbed on Cu(111). Imaging conditions: (C, D) 20 mV, 200 pA. Scale bars: 0.5 nm.

trates how the molecule can rotate around the N–Cu bond that forms the axel of the molecular rotor. Figure 1B shows a typical larger STM image with both isolated single molecules and small clusters present. For the purpose of this study on single-molecule rotors, only isolated molecules that were several nanometers from any neighboring molecules were examined. In the high-resolution images in Figure 1C,D, one can see from the individual rotating molecules that they are mirror images of one another and hence chiral. This observation indicates that, while enantiomers of N-methylbutylamine undergo fast interconversion in the gas phase, on the Cu(111) surface, binding of the lone pair of the N atom to Cu means that each enantiomer maintains its chirality. ^{45,46}

To further support these experimental findings, DFT calculations and STM image simulations were performed to interrogate the barrier to rotation and the appearance of the molecules in the STM images. DFT-derived energies along the rotational path shown in Figure 2A reveal that there is a very small barrier (14 meV) for a 60° rotation of the molecule around the N-Cu axel to the next equivalent stable orientation on the Cu(111) surface. This explains the pseudo-hexagonal shape of the individual molecules in the STM images that occur due to time averaging of the six equivalent stable orientations that the molecule rapidly switches between the slow timescale of STM imaging. Furthermore, the DFToptimized structures enabled us to make absolute assignments of the chirality of each absorbed molecule. Specifically, Figure 2B shows simulated STM images of the DFT-optimized structures in which the chirality of the adsorbed molecule can be directly seen in the image. Time averages of these projections over the six equivalent orientations of the molecule on Cu(111) yield pinwheel shapes that are in excellent agreement with the STM images of the rotating molecules. This allows us to use the Cahn-Ingold-Prelog rules for assigning chirality to label each isolated molecule as R or S.

To study electrical excitation of the single molecules' tunneling current versus time (I vs t), measurements were

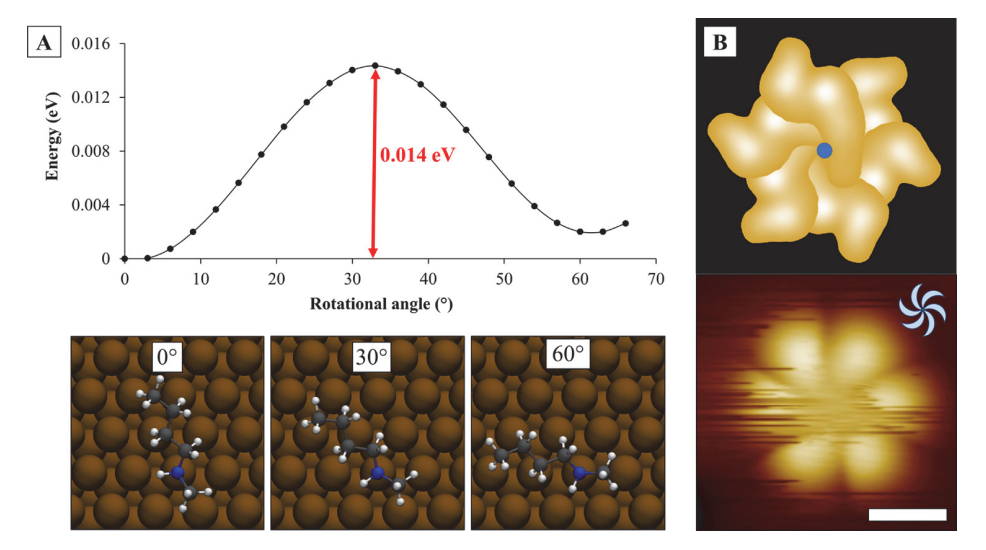


Figure 2. (A) DFT-derived energies as a function of the rotation angle for the optimized N-methylbutylamine geometry with the N atom atop a Cu atom. The rotation of this molecule by 60° was enough to cover the whole rotational path. The top-view schematic of N-methylbutylamine on Cu(111) at different angles of rotation is shown below the graph. (B) Simulated STM image of an S enantiomer rotor over six equivalent orientations of the molecule on Cu(111). The blue spot indicates the position of the N atom center. An STM image of the S enantiomer is shown below for comparison. Simulation STM conditions: 200 mV, 4.64 Å tip position. STM imaging conditions: 20 mV, 200 pA. Scale bar: 0.5 nm.

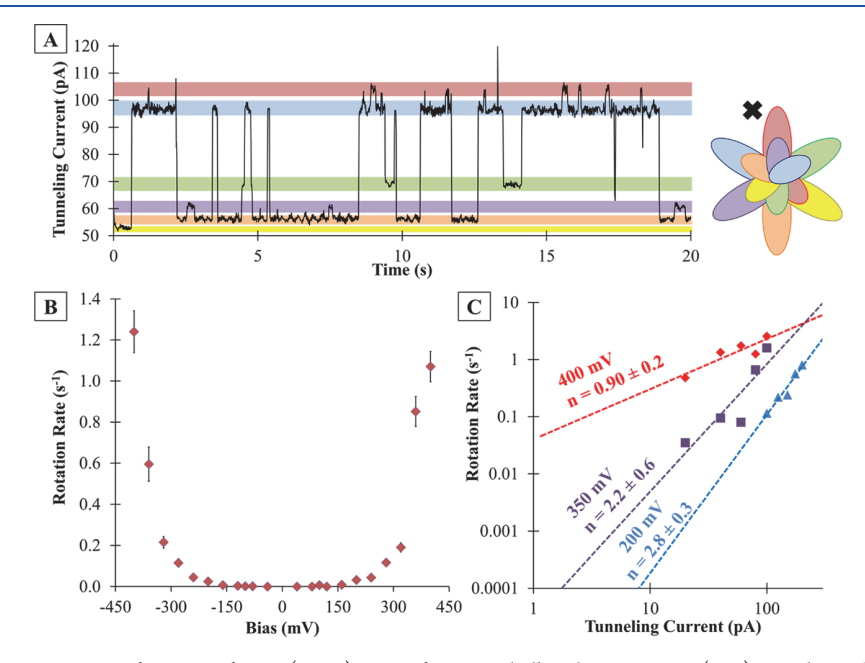


Figure 3. (A) Tunneling current as a function of time (I vs t) traces for N-methylbutylamine on Cu(111) reveals six discrete tunneling current values that correspond to the six inequivalent orientations of the molecule (red, blue, green, purple, orange, and yellow) with respect to the position of the STM tip position as marked by the black cross symbol. The larger lobes in the schematic indicate the butyl group position, while the smaller lobes indicate the methyl group position of the rotor. Excitation conditions: 400 mV, 100 pA. (B) Action spectra for N-methylbutylamine on Cu(111) at a set tunneling current of 10 pA showing a sharp increase in the rotation rate above the 360 mV threshold voltage, regardless of the positive/negative bias. (C) Plot of rotation rate vs tunneling current for various applied voltages. The lines are power law fits to the data; n gives the electron order, i.e., one vs multiple electron-induced rotation.

taken in which the STM tip is positioned off to the side of one of the lobes of the pinwheel shape of the rotating molecule with the feedback loop off and the tunneling current (I) recorded over time (t). As can be seen in Figure 3A, these traces show "long" periods where the molecule is in one orientation (i.e., one tunneling current value) separated by "fast" switching between the six different rotational orientations. These six tunneling currents correspond to the six

equivalent orientations of the alkyl tail (as shown in the schematic in Figure 3A where the STM tip position is marked with an "X"). These six tunneling current levels arise from the position of the molecular lobes with respect to the STM tip; the shorter the distance between the tip and rotor, the higher the tunneling current. These single-point measurements allow us to quantify rotation rates of single molecules. Furthermore, by recording these I versus t traces as a function of applied

voltage, it enables us to plot action spectra that relate the rate of an action (in this case, a rotation rate that refers to any molecular rotation between the six equivalent orientations) to the energy of the tunneling electrons (as defined by the voltage across the tunnel junction). The action spectrum in Figure 3B shows a sharp increase of the rotation rate around 360 mV, regardless of the direction of electron flow. This is a characteristic of inelastic electron tunneling by which an electron with an energy at or greater than the molecular vibration mode quanta it couples to can lead to the motion of the molecule as a whole. $^{47-49}$

To determine whether the electrical excitation of the rotational motion is a one- or multi-electron process, the tunneling current (I) dependence of the rotation rate (k) was studied, and the rotation rate is plotted as a function of the tunneling current

$$k = I^n$$

in which n refers to the number of electrons a given process involves. ⁴⁷ The results in Figure 3C show that, at or below 350 mV, rotational excitation is a multi-electron process versus a one-electron process at 400 mV. This, in conjunction with the action spectroscopy results that show a sharp increase in rotation rate at ~360 mV, indicates that the primary pathway for electrical excitation of the rotor occurs via excitation of C–H stretch modes that occur at this energy. ^{47,48} Excitation of the N–H mode of the molecule can be ruled out as N–H stretches in amines that occur in the range of 3300–3500 cm⁻¹, which would lead to an onset voltage of 410–430 meV. ⁵⁰

When comparing the energy input (360 meV electron) to the barrier to rotation in which DFT puts at \sim 14 meV, one can see that there is a significant difference in energy between the input and output channels. These barrier estimates and rotation rates are influenced by entropy effects and finite temperature corrections, 20 but such effects are less significant at low temperature and cannot account for a mismatch of over one order of magnitude. This mismatch between high-energy vibrational modes that drive the low energy rotational motion has been observed in molecular systems before and arises from the C-H vibrational modes having a high inelastic excitation cross section for excitation followed by energy transfer via anharmonic coupling of these high-energy vibrational modes to lower energy rotational and frustrated translational modes. 51-54 This also indicates that the rate of vibrational relaxation via energy transfer to the Cu(111) surface occurs slowly enough to allow the IVR coupling that leads the rotation to occur.^{54–59}

No evidence for preferential rotation in one direction was observed, which is consistent with symmetric rotation barriers in the DFT derived energies in Figure 2, and is in contrast with other surface-adsorbed molecules with asymmetric torsional barriers that produce net directionality in their rotation when electrically excited by STM tips. ^{27,60,61} However, when measuring the electrically induced rotation rates of the two enantiomers of the molecule under identical excitation conditions (i.e., same tunneling voltage, tunneling current, and sample temperature), statistically significant differences in the rotation rate of the two enantiomers of the molecule were observed. By changing the STM tip between measurements *via* high voltage pulses or surface indentation, some STM tips were observed to induce faster rotation of the *R* enantiomer of the rotor, while other tips induce faster rotation of the *S*

enantiomer, as seen in Figure 4A. To further demonstrate this effect, we studied six enantiomers of the molecules isolated

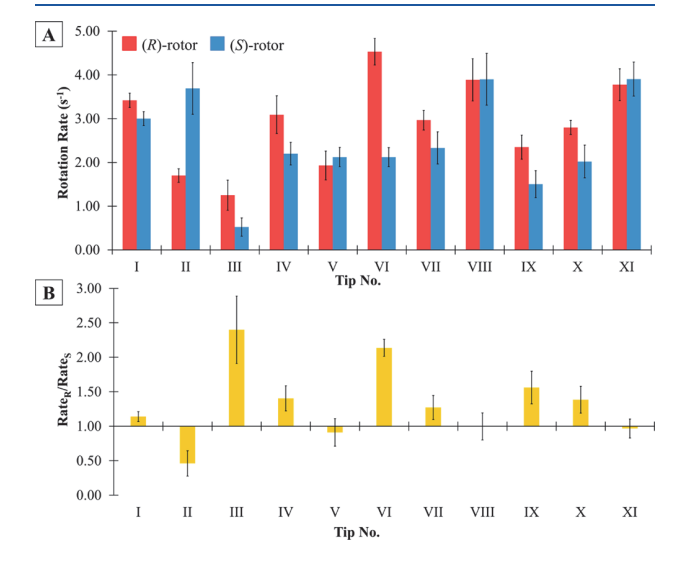


Figure 4. Plots of the (A) tunneling electron-induced rotation rate of R and S enantiomers of N-methylbutylamine with different STM tips; the R rotor is represented in red, and the S rotor is represented in blue. (B) Rotation rate ratios (Rate_R/Rate_S). Excitation conditions: 400 mV, 100 pA. Error bars reflect one standard deviation.

from each other in the same area of the surface with the same STM tip state. Specifically, Figure S3 demonstrates that the interaction of the STM tip with the three S enantiomers leads to a slow (\sim 2 Hz) rotation rate versus the same STM tip in the same tip state interacting with the R enantiomers, which leads to a faster (\sim 8 Hz) rate. This data definitively demonstrates that the interaction between the STM tip and the chiral molecules is different depending if the R or S enantiomer is probed and a classic diastereomeric relationship is observed.

Given that the rotational rate differences are physical properties of the system, the STM tip itself must be chiral to induce this diastereomerism. 27,62 To aid in this comparison, the ratio of the rotational rates (Rate_R/Rate_S) for different STM tips is shown in Figure 4B. Statistically significant ratios above 1.0 represent STM tips that are chiral and favor excitation of the *R* enantiomer, while ratios below 1.0 represent STM tips that favor excitation of the *S* enantiomer. Ratios closer to 1.00 come from STM tips with no measurable chirality as the rotation rate of both enantiomers is equal within error.

CONCLUSIONS

A combined STM and DFT study of a new molecular rotor system consisting of individual N-methylbutylamine molecules bound to a $\operatorname{Cu}(111)$ surface is reported. Rotation around the N–Cu bond gives increase to the chiral pinwheel appearance of individual rotating molecules, and our complementary DFT calculations enable the chirality of each individual molecular rotor to be assigned. The results presented indicate that the rotation of the molecules can be driven by tunneling electrons with an energy of 360 meV or greater in a one-electron process. Importantly, significant differences in the rotation rates of R and S enantiomers of the molecule were observed, and it was found that these differences change as the STM tip has changed. These results highlight the diastereomerism

arising from the interaction of a chiral STM tip and a chiral molecule. The fact that rates differing by >100% were observed between enantiomers indicate that care must be taken when interpreting results from systems that involve electrical contacts to single molecules like break junctions and scanning probe experiments as unforeseen chirality of the metal electrode (in this case, the STM tip) may lead to large differences in rates of induced motion in the different enantiomers of the molecule. Furthermore, in the future, it would be interesting to study how different STM tip etchings or cutting procedures affect the chirality of the STM tip as measured by differences in rotation rates between enantiomers and even the use of chiral etchant solutions that may yield tips of one chirality. However, given the serial nature of experiments, and the slow turnaround time for 5 K imaging experiments, this would take years of work to produce statistically significant data.

ASSOCIATED CONTENT

Supporting Information

The Supporting Information is available free of charge at https://pubs.acs.org/doi/10.1021/acs.jpcc.0c10767.

DFT calculations of the rotational barrier, simulated STM images for N-methylbutylamine on Cu(111), and control experiments for excitation of pairs of enantiomers (PDF)

AUTHOR INFORMATION

Corresponding Authors

Prashant Deshlahra — Department of Chemical and Biological Engineering, Tufts University, Medford, Massachusetts 02155, United States; ⊙ orcid.org/0000-0002-1063-4379; Email: prashant.deshlahra@tufts.edu

E. Charles H. Sykes — Department of Chemistry, Tufts University, Medford, Massachusetts 02155, United States; orcid.org/0000-0002-0224-2084; Email: charles.sykes@tufts.edu

Authors

Tedros A. Balema – Department of Chemistry, Tufts University, Medford, Massachusetts 02155, United States Yilang Liu – Department of Chemical and Biological Engineering, Tufts University, Medford, Massachusetts 02155, United States

Natalie A. Wasio — Department of Chemistry, Tufts University, Medford, Massachusetts 02155, United States Amanda M. Larson — Department of Chemistry, Tufts University, Medford, Massachusetts 02155, United States; orcid.org/0000-0002-0319-7326

Dipna A. Patel – Department of Chemistry, Tufts University, Medford, Massachusetts 02155, United States

Complete contact information is available at: https://pubs.acs.org/10.1021/acs.jpcc.0c10767

Notes

The authors declare no competing financial interest.

ACKNOWLEDGMENTS

The authors thank the U.S. National Science Foundation (Grant CHE-1708397) for support of the experimental work. Y.L. and P.D. acknowledge the support from the National Science Foundation (Award 1803798) and computational

resources from $XSEDE^{63}$ (Award ACI-1548562) for the theory work.

■ REFERENCES

- (1) Kelly, T. R.; Bowyer, M. C.; Bhaskar, K. V.; Bebbington, D.; Garcia, A.; Lang, F.; Kim, M. H.; Jette, M. P. A Molecular Brake. *J. Am. Chem. Soc.* **1994**, *116*, 3657–3658.
- (2) Baroncini, M.; Silvi, S.; Venturi, M.; Credi, A. Photoactivated Directionally Controlled Transit of a Non-Symmetric Molecular Axle through a Macrocycle. *Angew. Chem., Int. Ed.* **2012**, *51*, 4223–4226.
- (3) Li, H.; Cheng, C.; McGonigal, P. R.; Fahrenbach, A. C.; Frasconi, M.; Liu, W. G.; Zhu, Z.; Zhao, Y.; Ke, C.; Lei, J.; et al. Relative Unidirectional Translation in an Artificial Molecular Assembly Fueled by Light. *J. Am. Chem. Soc.* **2013**, *135*, 18609–18620.
- (4) Kassem, S.; Lee, A. T. L.; Leigh, D. A.; Markevicius, A.; Solà, J. Pick-up, Transport and Release of a Molecular Cargo Using a Small-Molecule Robotic Arm. *Nat. Chem.* **2016**, *8*, 138–143.
- (5) Astumian, R. D. Chemical Peristalsis. *Proc. Natl. Acad. Sci.* **2005**, 102, 1843–1847.
- (6) Kay, E. R.; Leigh, D. A.; Zerbetto, F. Synthetic Molecular Motors and Mechanical Machines. *Angew. Chem., Int. Ed.* **2007**, *46*, 72–191.
- (7) Hernández, J. V.; Kay, E. R.; Leigh, D. A. A Reversible Synthetic Rotary Molecular Motor. *Science* **2004**, *306*, 1532–1537.
- (8) Su, X.; Voskian, S.; Hughes, R. P.; Aprahamian, I. Manipulating Liquid-Crystal Properties Using a PH Activated Hydrazone Switch. *Angew. Chem., Int. Ed.* **2013**, *52*, 10734–10739.
- (9) Su, X.; Aprahamian, I. Switching around Two Axles: Controlling the Configuration and Conformation of a Hydrazone-Based Switch. *Org. Lett.* **2011**, *13*, 30–33.
- (10) Astumian, R. D. Running on Information. *Nat. Nanotechnol.* **2016**, *11*, 582–583.
- (11) Kottas, G. S.; Clarke, L. I.; Horinek, D.; Michl, J. Artificial Molecular Rotors. *Chem. Rev.* **2005**, *105*, 1281–1376.
- (12) Wintjes, N.; Bonifazi, D.; Cheng, F.; Kiebele, A.; Stöhr, M.; Jung, T.; Spillmann, H.; Diederich, F. A Supramolecular Multiposition Rotary Device. *Angew. Chem., Int. Ed.* **2007**, *46*, 4089–4092.
- (13) Huan, J.; Zhang, X.; Zeng, Q. Two-Dimensional Supramolecular Crystal Engineering: Chirality Manipulation. *Phys. Chem. Chem. Phys.* **2019**, *21*, 11537–11553.
- (14) Lischka, M.; Fritton, M.; Eichhorn, J.; Vyas, V. S.; Strunskus, T.; Lotsch, B. V.; Björk, J.; Heckl, W. M.; Lackinger, M. On-Surface Polymerization of 1,6-Dibromo-3,8-Diiodpyrene—A Comparative Study on Au(111) Versus Ag(111) by STM, XPS, and NEXAFS. *J. Phys. Chem. C* 2018, 122, 5967–5977.
- (15) Zheng, X.; Mulcahy, M. E.; Horinek, D.; Galeotti, F.; Magnera, T. F.; Michl, J. Dipolar and Nonpolar Altitudinal Molecular Rotors Mounted on an Au(111) Surface. *J. Am. Chem. Soc.* **2004**, *126*, 4540–4542.
- (16) Horinek, D.; Michl, J. Surface-Mounted Altitudinal Molecular Rotors in Alternating Electric Field: Single-Molecule Parametric Oscillator Molecular Dynamics. *Proc. Natl. Acad. Sci.* **2005**, *102*, 14175–14180.
- (17) Greber, T.; Šljivančanin, Ž.; Schillinger, R.; Wider, J.; Hammer, B. Chiral Recognition of Organic Molecules by Atomic Kinks on Surfaces. *Phys. Rev. Lett.* **2006**, *96*, No. 056103.
- (18) Karageorgaki, C.; Mutombo, P.; Jelinek, P.; Ernst, K.-H. Chiral Surface from Achiral Ingredients: Modification of Cu(110) with Phthalic Acid. *J. Phys. Chem. C* **2019**, *123*, 9121–9127.
- (19) Böhringer, M.; Morgenstern, K.; Schneider, W.-D.; Berndt, R. Separation of a Racemic Mixture of Two-Dimensional Molecular Clusters by Scanning Tunneling Microscopy. *Angew. Chem., Int. Ed.* **1999**, 38, 821–823.
- (20) Zhong, D.; Blömker, T.; Wedeking, K.; Chi, L.; Erker, G.; Fuchs, H. Surface-Mounted Molecular Rotors with Variable Functional Groups and Rotation Radii. *Nano Lett.* **2009**, *9*, 4387–4391.
- (21) Gehrig, J. C.; Penedo, M.; Parschau, M.; Schwenk, J.; Marioni, M. A.; Hudson, E. W.; Hug, H. J. Surface Single-Molecule Dynamics

- Controlled by Entropy at Low Temperatures. *Nat. Commun.* **2017**, *8*, 14404.
- (22) Lewis, E. A.; Murphy, C. J.; Liriano, M. L.; Sykes, E. C. H. Atomic-Scale Insight into the Formation, Mobility and Reaction of Ullmann Coupling Intermediates. *Chem. Commun.* **2014**, *50*, 1006–1008
- (23) Hersam, M. C.; Guisinger, N. P.; Lyding, J. W. Isolating, Imaging, and Electrically Characterizing Individual Organic Molecules on the Si(100) Surface with the Scanning Tunneling Microscope. *J. Vac. Sci. Technol., A* **2000**, *18*, 1349–1353.
- (24) Stöhr, M.; Wagner, T.; Gabriel, M.; Weyers, B.; Möller, R. Direct Observation of Hindered Eccentric Rotation of an Individual Molecule: Cu-Phthalocyanine on C60. *Phys. Rev. B* **2001**, *65*, No. 033404.
- (25) Ye, T.; Takami, T.; Wang, R.; Jiang, J.; Weiss, P. S. Tuning Interactions between Ligands in Self-Assembled Double-Decker Phthalocyanine Arrays. *J. Am. Chem. Soc.* **2006**, *128*, 10984–10985.
- (26) Wahl, M.; Stöhr, M.; Spillmann, H.; Jung, T. A.; Gade, L. H. Rotation–Libration in a Hierarchic Supramolecular Rotor–Stator System: Arrhenius Activation and Retardation by Local Interaction. *Chem. Commun.* **2007**, *2*, 1349–1351.
- (27) Tierney, H. L.; Murphy, C. J.; Jewell, A. D.; Baber, A. E.; Iski, E. V.; Khodaverdian, H. Y.; McGuire, A. F.; Klebanov, N.; Sykes, E. C. H. Experimental Demonstration of a Single-Molecule Electric Motor. *Nat. Nanotechnol.* **2011**, *6*, 625–629.
- (28) Baber, A. E.; Tierney, H. L.; Sykes, E. C. H. A Quantitative Single-Molecule Study of Thioether Molecular Rotors. *ACS Nano* **2008**, *2*, 2385–2391.
- (29) Jewell, A. D.; Tierney, H. L.; Baber, A. E.; Iski, E. V.; Laha, M. M.; Sykes, E. C. H. Time-Resolved Studies of Individual Molecular Rotors. *J. Phys. Condens. Matter* **2010**, *22*, 264006.
- (30) Tierney, H. L.; Han, J. W.; Jewell, A. D.; Iski, E. V.; Baber, A. E.; Sholl, D. S.; Sykes, E. C. H. Chirality and Rotation of Asymmetric Surface-Bound Thioethers. *J. Phys. Chem. C* **2010**, *115*, 897–901.
- (31) Tierney, H. L.; Baber, A. E.; Jewell, A. D.; Iski, E. V.; Boucher, M. B.; Sykes, E. C. H. Mode-Selective Electrical Excitation of a Molecular Rotor. *Chem. Eur. J.* **2009**, *15*, 9678–9680.
- (32) Kudernac, T.; Ruangsupapichat, N.; Parschau, M.; Maciá, B.; Katsonis, N.; Harutyunyan, S. R.; Ernst, K.-H.; Feringa, B. L. Electrically Driven Directional Motion of a Four-Wheeled Molecule on a Metal Surface. *Nature* **2011**, *479*, 208–211.
- (33) Zhang, Y.; Kersell, H.; Stefak, R.; Echeverria, J.; Iancu, V.; Perera, U. G. E.; Li, Y.; Deshpande, A.; Braun, K. F.; Joachim, C.; et al. Simultaneous and Coordinated Rotational Switching of All Molecular Rotors in a Network. *Nat. Nanotechnol.* **2016**, *11*, 706–712
- (34) Seldenthuis, J. S.; Prins, F.; Thijssen, J. M.; van der Zant, H. S. J. An All-Electric Single-Molecule Motor. *ACS Nano* **2010**, *4*, 6681–6686.
- (35) Neumann, J.; Gottschalk, K. E.; Astumian, R. D. Driving and Controlling Molecular Surface Rotors with a Terahertz Electric Field. *ACS Nano* **2012**, *6*, 5242–5248.
- (36) Jewell, A. D.; Tierney, H. L.; Zenasni, O.; Lee, T. R.; Sykes, E. C. H. Asymmetric Thioethers as Building Blocks for Chiral Monolayers. *Top. Catal.* **2011**, *54*, 1357–1367.
- (37) Astumian, R. D. Trajectory and Cycle-Based Thermodynamics and Kinetics of Molecular Machines: The Importance of Microscopic Reversibility. *Acc. Chem. Res.* **2018**, 2653.
- (38) Kresse, G.; Hafner, J. Ab Initio Molecular Dynamcis for Liquid Metals. *Phys. Rev. B* **1993**, 47, 558.
- (39) Kresse, G.; Furthmüller, J. Efficiency of Ab-Initio Total Energy Calculations for Metals and Semiconductors Using a Plane-Wave Basis Set. *Comput. Mater. Sci.* **1996**, *6*, 15–50.
- (40) Kresse, G.; Furthmüller, J. Efficient Iterative Schemes for Ab Initio Total-Energy Calculations Using a Plane-Wave Basis Set. *Phys. Rev. B* **1996**, *54*, 11169–11186.
- (41) Perdew, J. P.; Burke, K.; Ernzerhof, M. Generalized Gradient Approximation Made Simple. *Phys. Rev. Lett.* **1996**, 77, 3865–3868.

- (42) Kresse, G.; Joubert, D. From Ultrasoft Pseudopotentials to the Projector Augmented-Wave Method. *Phys. Rev. B* **1999**, *59*, 1758–1775.
- (43) Makov, G.; Payne, M. C. Periodic Boundary Conditions in Ab Initio Calculations. *Phys. Rev. B* **1995**, *51*, 4014–4022.
- (44) Hendrik, J. Monkhorst. Special Points Fro Brillouin-Zone Integretions. *Phys. Rev. B* **1976**, *13*, 5188–5192.
- (45) Lehn, J. M. Nitrogen Inversion. In *Dynamic Stereochemistry*; Springer-Verlag: Berlin/Heidelberg, 1970; pp. 311–377, DOI: 10.1007/BFb0050820.
- (46) Greenwood, N. N.; Earnshaw, A. Chemistry of the Elements, 2nd ed.; Elsevier Science: 1997.
- (47) Stipe, B. C.; Rezaei, M. A.; Ho, W. Single-Molecule Vibrational Spectroscopy and Microscopy. *Science* **1998**, *280*, 1732–1735.
- (48) Lauhon, L. J.; Ho, W. Control and Characterization of a Multistep Unimolecular Reaction. *Phys. Rev. Lett.* **2000**, *84*, 1527–1530.
- (49) Sainoo, Y.; Kim, Y.; Komeda, T.; Kawai, M. Inelastic Tunneling Spectroscopy Using Scanning Tunneling Microscopy on Trans-2-Butene Molecule: Spectroscopy and Mapping of Vibrational Feature. *J. Chem. Phys.* **2004**, *120*, 7249–7251.
- (50) Stewart, J. E. Vibrational Spectra of Primary and Secondary Aliphatic Amines. *J. Chem. Phys.* **1959**, *30*, 1259–1265.
- (51) Komeda, T.; Kim, Y.; Kawai, M.; Persson, B. N.; Ueba, H. Lateral Hopping of Molecules Induced by Excitation of Internal Vibration Mode. *Science* **2002**, 295, 2055–2058.
- (52) Ohara, M.; Kim, Y.; Yanagisawa, S.; Morikawa, Y.; Kawai, M. Role of Molecular Orbitals near the Fermi Level in the Excitation of Vibrational Modes of a Single Molecule at a Scanning Tunneling Microscope Junction. *Phys. Rev. Lett.* **2008**, *100*, 1–4.
- (53) Pascual, J. I.; Lorente, N.; Song, Z.; Conrad, H.; Rust, H.-P. Selectivity in Vibrationally Mediated Single-Molecule Chemistry. *Nature* **2003**, 423, 525–528.
- (54) Stipe, B. C.; Rezaei, M. A.; Ho, W. Coupling of Vibrational Excitation to the Rotational Motion of a Single Adsorbed Molecule. *Phys. Rev. Lett.* **1998**, *81*, 1263–1266.
- (55) Sainoo, Y.; Kim, Y.; Okawa, T.; Komeda, T.; Shigekawa, H.; Kawai, M. Excitation of Molecular Vibrational Modes with Inelastic Scanning Tunneling Microscopy Processes: Examination through Action Spectra of Cis-2-Butene on Pd(110). *Phys. Rev. Lett.* **2005**, 95, 1–4.
- (56) Parschau, M.; Passerone, D.; Rieder, K.-H.; Hug, H. J.; Ernst, K.-H. Switching the Chirality of Single Adsorbate Complexes. *Angew. Chem., Int. Ed.* **2009**, *48*, 4065–4068.
- (57) Violeta, S. M.; Meyer, J.; Morgenstern, K. Chirality Change of Chloronitrobenzene on Au(111) Induced by Inelastic Electron Tunneling. *Angew. Chem., Int. Ed.* **2009**, *48*, 4061–4064.
- (58) Stipe, B. C.; Rezaei, M. A.; Ho, W. Inducing and Viewing the Rotational Motion of a Single Molecule. *Science* **1998**, *279*, 1907–1909.
- (59) Sainoo, Y.; Kim, Y.; Komeda, T.; Kawai, M.; Shigekawa, H. Observation of Cis-2-Butene Molecule on Pd(110) by Cryogenic STM: Site Determination Using Tunneling-Current-Induced Rotation. *Surf. Sci.* **2003**, *536*, L403–L407.
- (60) Ernst, K.-H. A Turn in the Right Direction. *Nat. Nanotechnol.* **2013**, *8*, 7–8.
- (61) Zhang, Y.; Calupitan, J. P.; Rojas, T.; Tumbleson, R.; Erbland, G.; Kammerer, C.; Ajayi, T. M.; Wang, S.; Curtiss, L. A.; Ngo, A. T.; Ulloa, S. E.; Rapenne, G.; Hla, S. W. A Chiral Molecular Propeller Designed for Unidirectional Rotations on a Surface. *Nat. Commun.* **2019**, *10*, 3742.
- (62) Tierney, H. L.; Murphy, C. J.; Sykes, E. C. H. Regular Scanning Tunneling Microscope Tips Can Be Intrinsically Chiral. *Phys. Rev. Lett.* **2011**, *106*, No. 010801.
- (63) Towns, J.; Cockerill, T.; Dahan, M.; Foster, I.; Gaither, K.; Grimshaw, A.; Hazlewood, V.; Lathrop, S.; Lifka, D.; Peterson, G. D.; et al. XSEDE: Accelerating Scientific Discovery. *Comput. Sci. Eng.* **2014**, *16*, 62–74.